Loss of RAF kinase inhibitor protein is involved in myelomonocytic differentiation and aggravates *RAS*-driven myeloid leukemogenesis

Veronica Caraffini,[1] Olivia Geiger,[1] Angelika Rosenberger,[1] Stefan Hatzl,[1] Bianca Perfler,[1] Johannes L. Berg,[1] Clarice Lim,[2] Herbert Strobl,[2] Karl Kashofer,[3] Silvia Schauer,[3] Christine Beham-Schmid,[3] Gerald Hoefler,[3] Klaus Geissler,[4,5] Franz Quehenberger,[6] Walter Kolch,[7] Dimitris Athineos,[8] Karen Blyth,[8] Albert Wölfler,[1] Heinz Sill[1] and Armin Zebisch[1,9]

[1]Division of Hematology, Medical University of Graz, Graz, Austria; [2]Otto Loewi Research Center, Immunology and Pathophysiology, Medical University of Graz, Graz, Austria; [3]Diagnostic and Research Institute of Pathology, Medical University of Graz, Graz, Austria; [4]5th Medical Department with Hematology, Oncology and Palliative Medicine, Hospital Hietzing, Vienna, Austria; [5]Sigmund Freud University, Vienna, Austria; [6]Institute of Medical Informatics, Statistics and Documentation, Medical University of Graz, Graz, Austria; [7]Systems Biology Ireland and Conway Institute, University College Dublin, Dublin, Ireland; [8]Cancer Research UK Beatson Institute, Glasgow, UK and [9]Otto Loewi Research Center for Vascular Biology, Immunology and Inflammation, Division of Pharmacology, Medical University of Graz, Graz, Austria

 doi:10.3324/haematol.2018.209650

Received: October 21, 2018.

Accepted: May 15, 2019.

Pre-published: May 16, 2019.

Correspondence: *ARMIN ZEBISCH* - armin.zebisch@medunigraz.at

Loss of RAF kinase inhibitor protein is involved in myelomonocytic differentiation and aggravates *RAS*-driven myeloid leukemogenesis

Supplemental data

Veronica Caraffini,[1] Olivia Geiger,[1] Angelika Rosenberger,[1] Stefan Hatzl,[1] Bianca Perfler,[1] Johannes L. Berg,[1] Clarice Lim,[2] Herbert Strobl,[2] Karl Kashofer,[3] Silvia Schauer,[3] Christine Beham-Schmid,[3] Gerald Hoefler,[3] Klaus Geissler,[4,5] Franz Quehenberger,[6] Walter Kolch,[7] Dimitris Athineos,[8] Karen Blyth,[8] Albert Wölfler,[1] Heinz Sill[1] and Armin Zebisch[1]

[1]Division of Hematology, [2]Otto Loewi Research Center, Immunology and Pathophysiology, [3]Diagnostic and Research Institute of Pathology, Medical University of Graz, Graz, Austria; [4]5th Medical Department with Hematology, Oncology and Palliative Medicine, Hospital Hietzing, Vienna, Austria; [5]Sigmund Freud University, Vienna, Austria; [6]Institute of Medical Informatics, Statistics and Documentation, Medical University of Graz, Graz, Austria; [7]Systems Biology Ireland & Conway Institute, University College Dublin, Dublin, Ireland; [8]Cancer Research UK Beatson Institute, Glasgow, United Kingdom

Supplemental materials and methods

Preparation of primary patient specimens

Peripheral blood or bone marrow from CMML patients was diluted with the same volume of phosphate buffered saline (PBS), carefully layered over Lymphoprep solution (Axis-Shield) and centrifuged at 2500 r.p.m. for 20 min at room temperature. Mononuclear cells and/or granulocytes were collected from the corresponding interface and subsequently cryopreserved in pellets of 3-5 x 10^7 cells in RPMI 1640 (Sigma) supplemented with 20% dimethyl sulphoxide (WAK-Chemie) and 10% human albumin (Octapharma) at -192°C. All samples contained at least 80% myelomonocytic cells as determined by Giemsa–May-Grünwald-stained cytospin preparations.

Analysis of mice

Mice with a complete deletion of *Rkip* (*Rkip-/-)* as well as their controls (*Rkip*+/+) were electively killed and analyzed at an age of 3, 6, 9 and 12 months. For *Mx1-Cre/Nras/Rkip-/-* and *Mx1-Cre/Nras/Rkip*+/+ genotypes, respectively, *Nras*-mutation was activated by intraperitoneal injections of polyinosinic polycytidilic acid (pIpC, Sigma; three times 250µg/d at every alternate day, starting at an age of 30 days). Then, mice were sacrificed and analyzed at day 180 after the first pIpC injection. *Nras/Rkip*+/+ mice were sacrificed at the same age. For in-vivo differentiation experiments, GM-CSF (Peprotech) was injected intraperitoneally in two months old mice (500ng twice daily, day 1-4) and analysis was performed on day 5. For survival analyses, mice were observed for signs of disease and were killed when moribund with each group comprising at least eleven animals.

Mice were sacrificed by cervical dislocation after anesthesia with isoflurane (4%). Cardiac blood was obtained in Microvet EDTA tubes (BD Biosciences) for complete blood cell counts using V-sight (Menarini diagnostics), for Giemsa (Merck) stained peripheral blood smears and for flow cytometry. Additionally, bone marrow, spleen, liver, lymph nodes, thymus as well as other abnormal organs and/or tumors were collected. They were measured as reported earlier[1] and additionally subjected to flow cytometry as well histology and immunohistochemistry. Additionally, cells from a peritoneal cavity lavage were collected and subjected to flow cytometry as outlined in detail below. For analysis of the activation of the *RAS*-MAPK/ERK signaling pathway, $CD11b^+$ cells were isolated from the bone marrow of *Rkip-/-* and *Mx1-Cre/Nras/Rkip-/-* mice*,* as well as from their controls *(Rkip*+/+ and *Mx1-Cre/Nras/Rkip*+/+*,* respectively) using anti-CD11b magnetic particles (BD biosciences), according to the manufacturer's protocol.

In-vitro differentiation assays

$CD34^+$ human HSPCs of six healthy donors were transduced with a GFP-tagged RKIP shRNA construct and treated with a cytokine mix comprising GM-CSF, FL, SCF and TNFa

for 5 days as previously described.[2] Myelomonocytic expression was assessed by CD11b and CD14 expression. To ensure that only successfully transduced cells were evaluated, additional gating for GFP positive cells was performed. For measuring the effects of 1,25-Dihydroxyvitamin D_3 ($1,25D_3$; Sigma) induced myelomonocytic differentiation of HL-60 cells on RKIP expression levels, HL-60 were treated with $1,25D_3$ at a concentration of 100nM for 48 hours. For measuring the effects of RKIP modulation on $1,25D_3$ induced differentiation, HL-60 were transfected with the constructs indicated in the main text of the manuscript. After 24h, cells were treated with 10nM $1,25D_3$ for another 48h and then screened for the expression of CD11c. For analysis of *RAS*-pathway activation in HL-60, cells were stably transduced with a lentiviral expression construct (psi-LVRU6GP, Genecopeia) and then starved for 24 hours in RPMI 1640 (Sigma) supplemented with 0.05% FCS.

Immunoblot analysis

Cell pellets were lysed using ice-cold RIPA-Buffer (Sigma-Aldrich) supplemented with protease and phosphatase inhibitor cocktails (Sigma-Aldrich and Thermo Fisher Scientific). Immunoblots were then performed as previously described[3] employing Mini-PROTEAN TGX gels for electrophoresis (Bio-Rad) and the Bio-Rad Trans Blot TurboBlotting System for transfer. Polyvinylidene difluoride membranes (Bio-Rad) were incubated with anti-RKIP (Merck Millipore), anti-GFP-RKIP (Cell Signaling), anti-ERK (Sigma-Aldrich), anti-pERK (Cell Signaling), anti–β-actin (Sigma-Aldrich) and anti-Vinculin (Abcam). The intensity of the bands was compared using ImageJ.[4] RKIP loss in CMML patient samples was defined as previously reported for AML.[3]

RNA extraction, reverse transcription and real time quantitative PCR

RNA was isolated from primary CMML patient samples using TRIzol (Thermo Fisher Scientific), and from hematopoietic cells of healthy donors as well as from umbilical cord blood employing the miRNAeasy Micro Kit (Qiagen) following the manufacturer´s instruction. cDNA synthesis was performed with TaqMan Reverse Transcription (RT) Reagents (Applied Biosystems) starting from 400 ng of total RNA and using random hexamers for RT. An Applied Biosystems 7500 Real-Time PCR System (Applied Biosystems) and the SYBR Green method (Invitrogen) were used for real time quantitative PCR (qPCR) for RKIP mRNA expression analysis. B2M and GAPDH were selected as control genes for the analyses performed and NB4 AML cells served as calibrator. The expression levels were evaluated employing the comparative ddCT method as previously described.[3]

Next-Generation Sequencing

Next-Generation Sequencing (NGS) was performed using an Ion Torrent Sequencing platform, as described previously.[5–8] The gene list analyzed included 39 genes with recurrent mutations in myeloid neoplasms: *CEBPA* (full coding); *NPM1* (Exon 11); *FLT3* (Exon 14-

16,20,21); *ASXL1* (Exon 12); *BCOR* (full coding); *BRAF* (Hotspot Exon 15); *CALR* (Exon 9); *CBL* (Exon 8,9); *CSF3R* (Exon 14-17); *DDX41* (full coding); *DNMT3a* (full coding); *ETNK1* (Exon 3); *ETV6* (full coding); *EZH2* (Exon 16-19); *GATA2* (full coding); *IDH1* (Exon 4); *IDH2* (Exon 4); *JAK2* (Exon 13); *KIT* (Exons 8,10,11,17); *KRAS* (Exon 2,3); *MPL* (Exon 10); *NF1* (full coding); *NRAS* (Exon 2,3); *PHF6* (full coding); *PTPN11* (Exon 3,13); *RUNX1* (Exon 3-8); *SETBP1* (Hotspot Exon 4); *SF3B1* (Exon 14-16); *SF3B2* (full coding); *SFRP1* (full coding); *SRP72* (full coding); *SRSF2* (Hotspot Exon 1); *STAG2* (full coding); *STAT3* (Exon 20,21); *TET2* (Exon 3-11); *TP53* (full coding); *U2AF1* (Exon 2,7,9); *WT1* (Exon 7,9); *ZRSR2* (full coding). Mutation calling necessitated a coverage of at least 1000x, a frequency in the 1000-genome project of <0.01% and a variant allele frequency (VAF) >10%.

Flow cytometry

Flow cytometry was performed as previously described using the following antibody panels: efluor-CD11b (eBiosciences), PE-Cy7-Ly6G (eBiosciences), APC-CD117 (eBiosciences) and 7-AAD (BD Pharmingen) for all phenotypic analyses of *Mx1-Cre/Nras/Rkip-/-* mice as well as for GM-CSF induced differentiation assays. CD11b-PECy7 (Biolegend), CD14-PE (Thermo Fisher eBioscience) and 7-AAD for the analysis of differentiation experiments in healthy umbilical cord blood HSPCs. PE-CD11c (Beckman Coulter) and 7-AAD (BD Pharmingen) for the analysis of differentiation experiments in HL-60 cells. For the phenotypic analysis of *Rkip-/-* animals, a myeloid panel comprising 7-AAD, FITC-CD11b and PE-CD115 (all eBioscience) as well as a lymphoid panel comprising 7-AAD, FITC-CD3e, PE-Cy7-CD49b (all eBioscience) and PE-CD45R/B220 (BD Pharmingen) were employed. Additionally, Biotin mouse lineage panel (BD Pharmingen), PE-Cy7 Sca-1, PE-CD115, PE-Cy5-CD135, APC-CD117, efluor-CD16/32, efluor-CD34 (all eBioscience) and 7-AAD (BD Pharmingen) were used to analyze hematopoietic progenitor cell compartments in these mice. Flow cytometric analyses were performed employing LSRII and FACSCalibur machines (both BD Biosciences). Data were analyzed using Kaluza software (Beckman Coulter).

Supplemental tables

		WBC (10^3/µl) [median]	Hb (g/dl) [median]	Hct (%) [median]	PLT (10^3/µl) [median]
3 months	***Rkip+/+***	4.36-12.02 [7.49] n=10	14.1-16.4 [14.8] n=10	43.4-49.9 [45.0] n=10	469.0-979.0 [634.5] n=10
	Rkip-/-	6.88-11.58 [10.35] n=9	13.1-16.1 [15] n=9	19.8-49.5 [45.8] n=9	211.0-665.0 [485.0] n=9
		P = 0.182	*P* = 0.604	*P* = 0.720	*P* = 0.095
6 months	***Rkip+/+***	4.59-13.81 [9.06] n=10	13.1-16.4 [15.3] n=10	43.8-56.0 [51.9] n=10	716.0-1214.0 [880.5] n=10
	Rkip-/-	8.28-19.46 [11.78] n=9	13.4-17.0 [15.2] n=9	46.2-59.1 [53.7] n=9	605.0-1126.0 [926.0] n=9
		P = 0.079	*P* = 0.780	*P* = 0.356	*P* = 0.780
9 months	***Rkip+/+***	3.58-12.03 [9.11] n=10	14.4-16.8 [15.5] n=10	42.8-50.3 [47.8] n=10	378.0-1599.0 [864.5] n=10
	Rkip-/-	7.24-15.71 [9.56] n=9	13.0-16.2 [14.9] n=9	42.9-51.1 [48.3] n=9	436.0-1268.0 [798.0] n=9
		P = 0.447	*P* = 0.079	*P* = 0.720	*P* = 0.604
12 months	***Rkip+/+***	4.78-12.2 [6.17] n=8	14.0-15.6 [14.4] n=8	31.6-47.7 [43.0] n=8	588.0-940.0 [787.0] n=8
	Rkip-/-	6.16-14.11 [10.36] n=9	12.5-17.1 [14.6] n=9	38.6-49.7 [44.4] n=9	409.0-1984.0 [926.0] n=9
		P = 0.068	*P* = 0.633	*P* = 0.146	*P* = 0.034

Supplemental Table 1. Results of the blood counts performed in 3, 6, 9 and 12 months old *Rkip*-/- mice as well as in age-matched control mice (*Rkip*+/+). The table presents ranges, the respective medians are depicted in square brackets. P-values were calculated employing the Student´s t-test. WBC, white blood cells; Hb, hemoglobin; Hct, hematocrit; PLT, platelets.

	WBC (10^3/µl) [median]	Hb (g/dl) [median]	Hct (%) [median]	PLT (10^3/µl) [median]
Nras/Rkip+/+	4.60-9.70 [6.80] n=5	9.20-15.50 [15.20] n=5	30.50-49.20 [48.50] n=5	454.00-1952.00 [1214.00] n=5
Mx1-Cre/Nras/Rkip+/+	5.80-8.65 [6.70] n=3	6.80-12.60 [11.90] n=3	24.90-41.50 [38.80] n=3	99.00-1106.00 [865.00] n=3
Mx1-Cre/Nras/Rkip-/-	9.78-14.57 [10.42] n=4	13.60-19.40 [14.00] n=4	39.30-60.00 [39.85] n=4	289.00-1368.00 [948.00] n=4
Nras/Rkip+/+ **vs** ***Mx1-Cre/Nras/Rkip-/-***	*P* = 0.017	*P* = 0.961	*P* = 0.532	*P* = 0.449
Mx1-Cre/Nras/Rkip+/+ **vs** ***Mx1-Cre/Nras/Rkip-/-***	*P* = 0.036	*P* = 0.248	*P* = 0.085	*P* = 0.622

Supplemental Table 2. Results of the blood counts from *Nras/Rkip*+/+, *Mx1-Cre/Nras/Rkip*+/+ as well as *Mx1-Cre/Nras/Rkip*-/- mice. The blood counts were performed at 180 days after the first pIpC injection. The table presents ranges, respective medians are depicted in square brackets. P-values were calculated employing the Student´s t-test. WBC, white blood cells; Hb, hemoglobin; Hct, hematocrit; PLT, platelets.

Genotype	Mouse ID	WBC (10^3/µl)	Hb (g/dl)	Hct (%)	PLT (10^3/µl)	HS	MP	MPD
Mx1-Cre/Nras/Rkip+/+	**#1121**	7.90	15.70	48.60	1421.00	++	+	-
Mx1-Cre/Nras/Rkip+/+	**#1249**	28.40	12.00	40.00	2029.00	++	++	+
Mx1-Cre/Nras/Rkip+/+	**#1301**	6.20	15.10	48.60	1329.00	++	+	-
Mx1-Cre/Nras/Rkip+/+	**#1455**	5.40	14.40	47.50	1170.00	+	++	-
Mx1-Cre/Nras/Rkip-/-	**#1139**	84.30	8.20	26.90	321.00	+	+++	+
Mx1-Cre/Nras/Rkip-/-	**#1176**	11.30	11.60	37.40	837.00	++	++	+
Mx1-Cre/Nras/Rkip-/-	**#1134**	80.10	14.30	45.50	124.00	+	+++	+
Mx1-Cre/Nras/Rkip-/-	**#1278**	28.60	14.50	46.70	1788.00	+	+++	+
Mx1-Cre/Nras/Rkip-/-	**#1434**	15.20	14.80	45.60	1120.00	+	++	+
Mx1-Cre/Nras/Rkip-/-	**#1263**	23.30	14.00	44.00	1481.00	++	+++	+
Mx1-Cre/Nras/Rkip-/-	**#1342**	23.40	12.20	37.70	1454.00	+	+++	+

Supplemental Table 3. Results of the blood counts as well as of the histopathologic evaluation of *Mx1-Cre/Nras/Rkip*+/+ and *Mx1-Cre/Nras/Rkip*-/- moribund mice. The table presents the blood counts of the analyzed animals (WBC, white blood cells; Hb, hemoglobin; Hct, hematocrit; PLT, platelets). In addition, the presence and severity of histiocytic sarcoma (HS), myeloproliferation (MP) and myeloproliferative disease (MPD), respectively, is displayed. In more detail, MPD was defined as either present (+) or absent (-), as defined previously.[9] For grading the extension of MP, we used a slightly adapted scoring system from Lacroix-Triki et al.,[10] where the average amount of hematopoietic foci per one 100x field was evaluated in the liver and spleen and scored as follows: 0 = absent, + = 1-2 hematopoietic foci, ++ = 3-4 hematopoietic foci and +++ = >4 hematopoietic foci. For HS, we used a scoring system, which includes both the amount of organs infiltrated and the extension of organ infiltration. Due to the absence of a previously established protocol, we thereby routinely analysed bone marrow, spleen, liver, lymph nodes and the thymus for the presence of HS (as defined by the Bethesda classification of nonlymphoid hematopoietic neoplasms in mice).[9] As organ infiltration was either very low or very high in all samples studied, we arbitrarily defined extensive infiltration of an organ, when more than 50% HS infiltration was present. Due to a generally lower infiltration rate, this cut-off was lowered to >30% infiltration in the liver. Subsequently, the extension of HS was defined as follows: 0 = no HS in any of the organs, "+" = HS present, but extensive organ infiltration in <3 of the 5 organs studied; "++" = extensive organ infiltration in ≥3 of the 5 organs studied.

	total	RKIP loss	RKIP normal	p-value
n	41/41 (100%)	12/41 (29%)	29/41 (71%)	
Age at diagnosis (y)	69 (54-85)	72 (60-85)	67 (54-84)	0.180
Sex				0.734
male (n)	23/41 (56%)	6/12 (50%)	17/29 (59%)	
female (n)	18/41 (44%)	6/12 (50%)	12/29 (41%)	
MMC (%)	79 (27-96)	86 (80-91)	76 (27-96)	0.030
AML transformation (n)	23/41 (56%)	8/12 (66%)	15/29 (52%)	0.497
Karyotype				0.458
normal (n)	22/27 (81%)	6/6 (100%)	16/21 (76%)	
-7 (n)	1/27 (4%)	0/6 (0%)	1/21 (5%)	
+8 (n)	3/27 (11%)	0/6 (0%)	3/21 (14%)	
complex	1/27 (4%)	0/6 (0%)	1/21 (5%)	
Therapy				0.471
BSC	22/37 (60%)	5/10 (50%)	17/27 (63%)	
HMA	12/37 (32%)	5/10 (50%)	7/27 (26%)	
low-dose AraC	2/37 (5%)	0/10 (0%)	2/27 (7%)	
Allo-SCT	1/37 (3%)	0/10 (0%)	1/27 (4%)	

Supplemental Table 4. Clinical characteristics of the 41 CMML primary patient samples analyzed. For age and myelomonocytic cells (MMC), the table presents the median with ranges in parentheses. BSC, best supportive care; HMA, hypomethylating agents; AraC, cytarabine; Allo-SCT, allogeneic stem cell transplantation. P-values were calculated by Wilcoxon-Mann-Whitney test for all continuous variables and by Fisher´s exact test for all dichotomous variables.

Patient	Gene	Nucleotide change	Amino acid change
#1	*NRAS*	c.G35A	p.G12D
#2	*NRAS*	c.G35A	p.G12D
#3	*NRAS*	c.G35A	p.G12D
	KRAS	c.G34A	p.G12S
#4	*KRAS*	c.G35T	p.G12V
#5	*KRAS*	c.C176G	p.A59G
#13	*NRAS*	c.G38A	p.G13D
#14	*NRAS*	c.G38A	p.G13D
#15	*NRAS*	c.G35A	p.G12D
#16	*NRAS*	c.G34A	p.G12S
#17	*KRAS*	c.A182G	p.Q61R
#18	*KRAS*	c.G35C	p.G12A
#19	*KRAS*	c.G57T	p.L19F
#20	*KRAS*	c.G34A	p.G12S

Supplemental Table 5. Detailed list of *RAS* mutations identified within this study. The "patient" column refers to patients with either RKIP loss or RKIP normal listed in Figure 8.

Supplemental figures

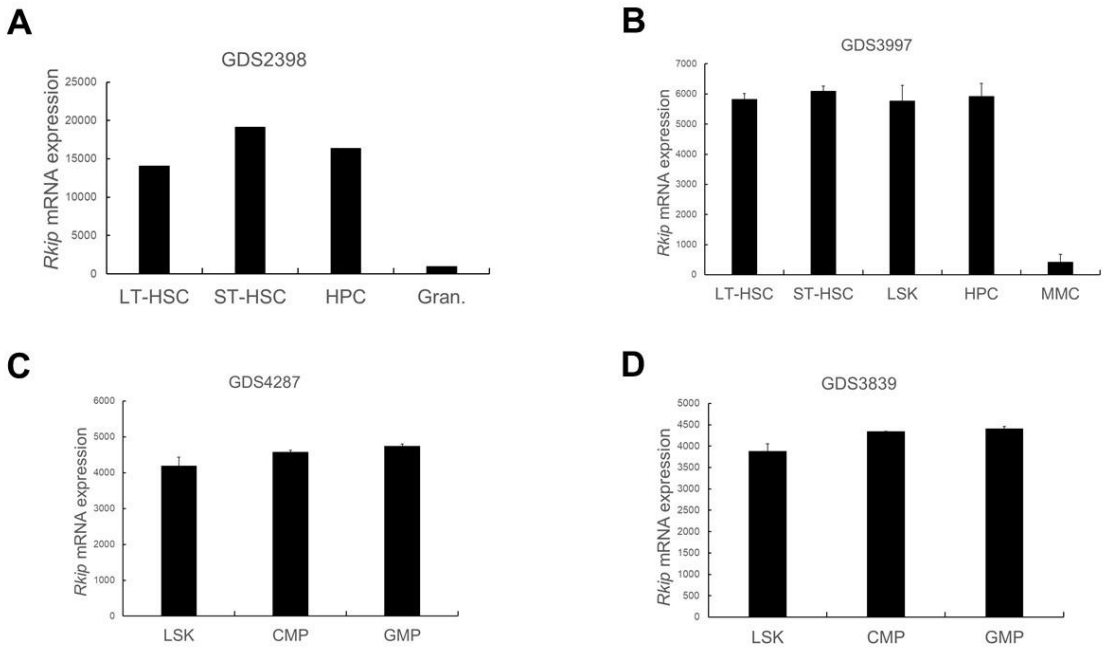

Supplemental Figure 1. *Rkip* expression during myelomonocytic differentiation. Microarray expression data for murine *Rkip* mRNA expression were downloaded and analyzed via the Gene Expression Omnibus (https://www.ncbi.nlm.nih.gov/geo/). (A) *Rkip* expression in LT-HSC (lin^-, Sca^+, kit^+, $CD34^-$), ST-HSC (lin^-, Sca^+, kit^+, $CD34^+$), HPC (lin^-, Sca^-, kit^+) and granulocytes (Gran.; based on SSC sorting and $Gr1^{high}$). Data were downloaded from Sung LY et al., GEO accession number GSE5677, GDS2398.[11] (B) *Rkip* expression in LT-HSC (lin^-, Sca^+, kit^+, $CD34^-$), ST-HSC (lin^-, Sca^+, kit^+, $CD34^+$), LSK (lin^-, Sca^+, kit^+), HPC (lin^-) and myelomonocytic cells (MMC, Gr-1^+ neutrophils and Mac-1^+ monocytes/macrophages). Data were downloaded from Konuma T et al., GEO accession number GSE27787, GDS3997.[12] (C) *Rkip* expression in LSK (lin^-, Sca^+, kit^+), CMP (lin^-, Sca^-, kit^+, $Fc\gamma R^{lo}$, $CD34^+$) and GMP (lin^-, Sca^-, kit^+, $Fc\gamma R^+$, $CD34^+$). Data were downloaded from Moran-Crusio K et al., GEO accession number GSE27816, GDS4287.[13] (D) *Rkip* expression in LSK (lin^-, Sca^+, kit^+), CMP (lin^-, Sca^-, kit^+, $Fc\gamma R^{lo}$, $CD34^+$) and GMP (lin^-, Sca^-, kit^+, $Fc\gamma R^+$, $CD34^+$). Data were downloaded from Wang Y et al., GEO accession number GSE20377, GDS3839.[14] LT-HSC, long-term hematopoietic stem cells; ST-HSC, short-term hematopoietic stem cells; HPC, hematopoietic progenitor cells; MMC, myelomonocytic cells; CMP, common myeloid progenitor; GMP, granulocyte-macrophage progenitor.

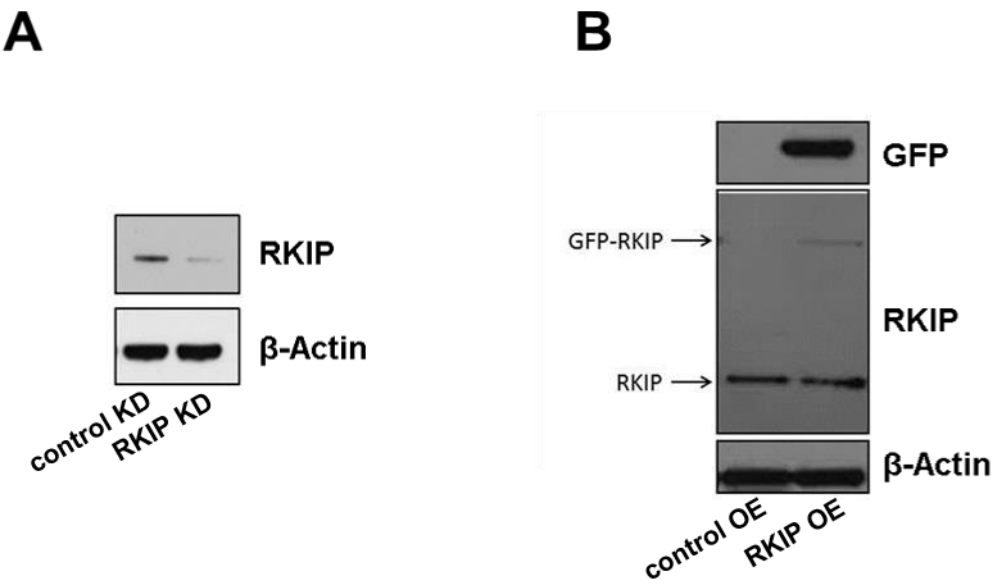

Supplemental Figure 2. RKIP knockdown/overexpression in HL-60 differentiation assays. As shown in Figure 2 B-C of the main manuscript, HL-60 cells were transfected with the indicated constructs. After 24h, cells were treated with 10nM $1,25D_3$ for another 48h and then screened for the expression of CD11c. The Immunoblots in Figure 2 B-C of the main manuscript show the successful knockdown/overexpression at the end of the indicated $1,25D_3$/control incubation period. In this supplemental figure, the extent of knockdown (A) and overexpression (B), respectively, at the beginning of the $1,25D_3$/control incubation period is shown.

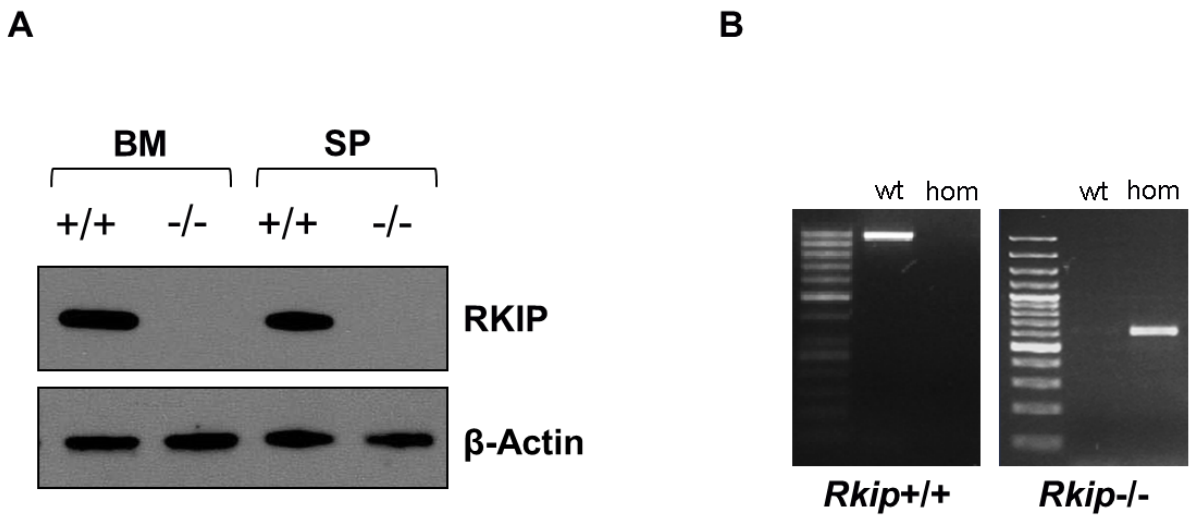

Supplemental Figure 3. Characterization of the RKIP murine model. (A) Immunoblot showing the complete deletion of Rkip in bone marrow (BM) and spleen (SP) of *Rkip*-/- mice. (B) Genotyping was performed in *Rkip*-/- mice as well as in control mice (*Rkip*+/+) by tail clipping, as previously described.[15,16]

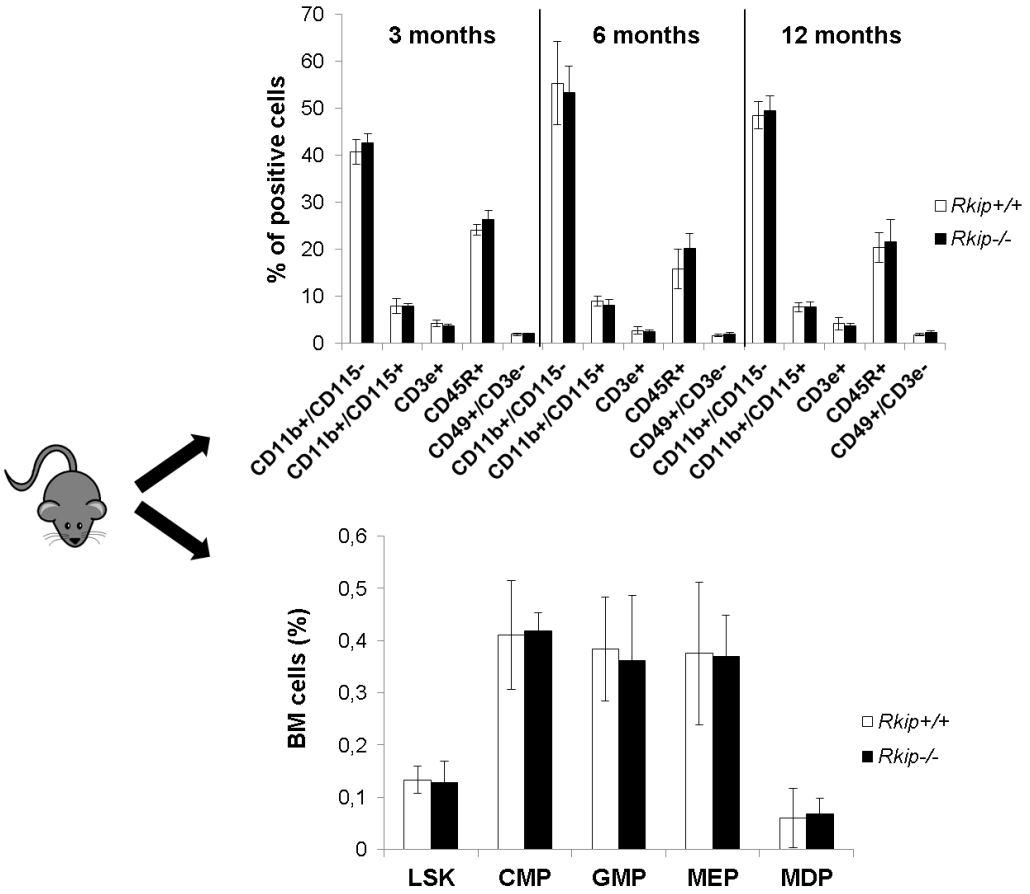

Supplemental Figure 4. Characterization of *Rkip-/-* mice. *Rkip-/-* mice, as well as control mice, were electively sacrificed at an age of 3, 6 and 12 months. No significant differences could be observed comparing *Rkip-/-* with *Rkip+/+* mice, both in the composition of leukocytes in peripheral blood (upper graph) on the one hand, and of hematopoietic progenitor compartments in BM on the other hand (graph below). LSK (lin^-, Sca^+, kit^+); CMP (common myeloid progenitor, lin^-, Sca^-, kit^+, $FcγR^{lo}$, $CD34^+$); GMP (granulocyte macrophage progenitor, lin^-, Sca^-, kit^+, $FcγR^+$, $CD34^+$); MDP (macrophage dendritic cell progenitor, lin^-, Sca^-, kit^+, $CD115^+$, $CD135^+$); MEP (megakaryocyte erythrocyte progenitor, lin^-, Sca^-, kit^+, $FcγR^{lo}$, $CD34^-$). Graphs denote the average of at least four independent experiments +/- SD, statistical significance was calculated using Student´s t-test.

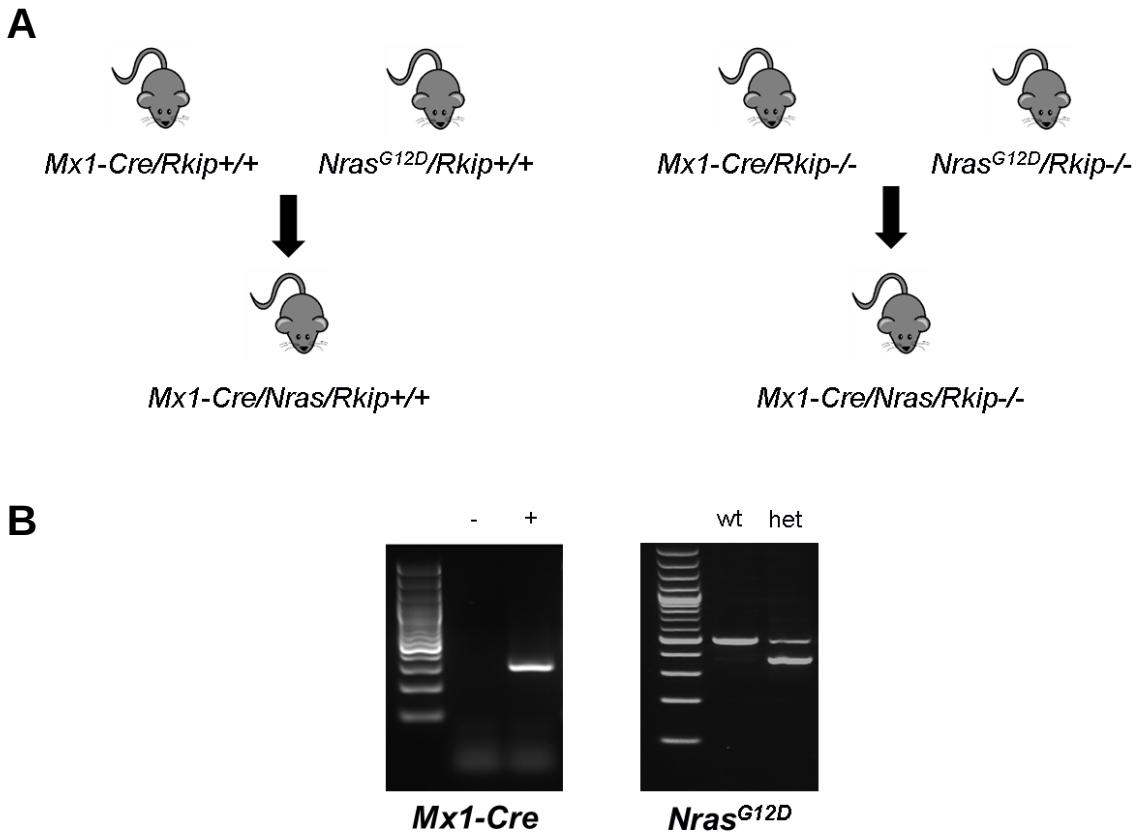

Supplemental Figure 5. Characterization of the *Nras*-mutated murine model. (A) To test the effects of *Rkip* loss on an *Nras*-mutated mice model, the breeding strategy depicted in the picture was used. (B) Representative PCR-gels from genotyping for *Mx1-Cre* and *Nras*^{G12D}. A homozygous situation was avoided for both genotypes. Genotyping for *Rkip* is presented in supplemental Figure 3.

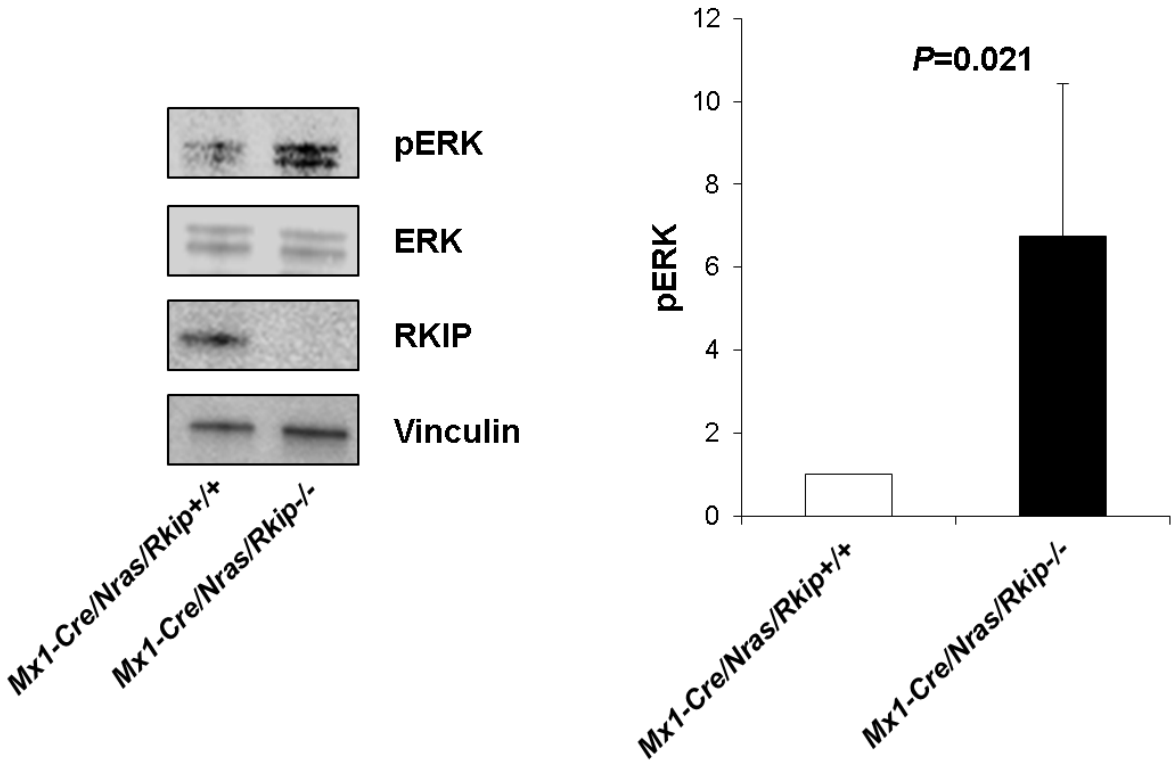

Supplemental Figure 6. Effects of *Rkip* deletion on pERK in *Mx1-Cre/Nras/Rkip-/-* mice after GM-CSF stimulation. CD11b^{+} cells of *Mx1-Cre/Nras/Rkip-/-* mice do not show increased baseline ERK phosphorylation, but hyper-respond to cytokine stimulation.[17] Figure 6D of the main manuscript shows an increase of pERK levels in *Mx1-Cre/Nras/Rkip-/-* mice without the addition of cytokines, which suggests that *Rkip* deletion increases pERK independently of mutated *Nras*. To study the effects of *Rkip* deletion on *RAS*-MAPK/ERK signaling under GM-CSF stimulation, CD11b^{+} cells of *Mx1-Cre/Nras/Rkip-/-* mice were isolated in absence of FCS and stimulated with 10 ng/ml GM-CSF in serum-free HBSS media for 15 minutes. Importantly, *Rkip* deletion increased ERK phosphorylation under these conditions as well. These data indicate that in addition to its role as independent *RAS*-MAPK/ERK regulator, *Rkip* deletion also increases the hyper-responsiveness of *Nras* mutated animals to GM-CSF stimulation. A representative immunoblot is presented on the left side, the graph denotes the average +/- SD; pERK intensity is given as x-fold change to the *Mx1-Cre/Nras/Rkip+/+* control genotype. Mice experiments were performed using n=3 mice for each genotype. Statistical significance was evaluated using Student's t-test.

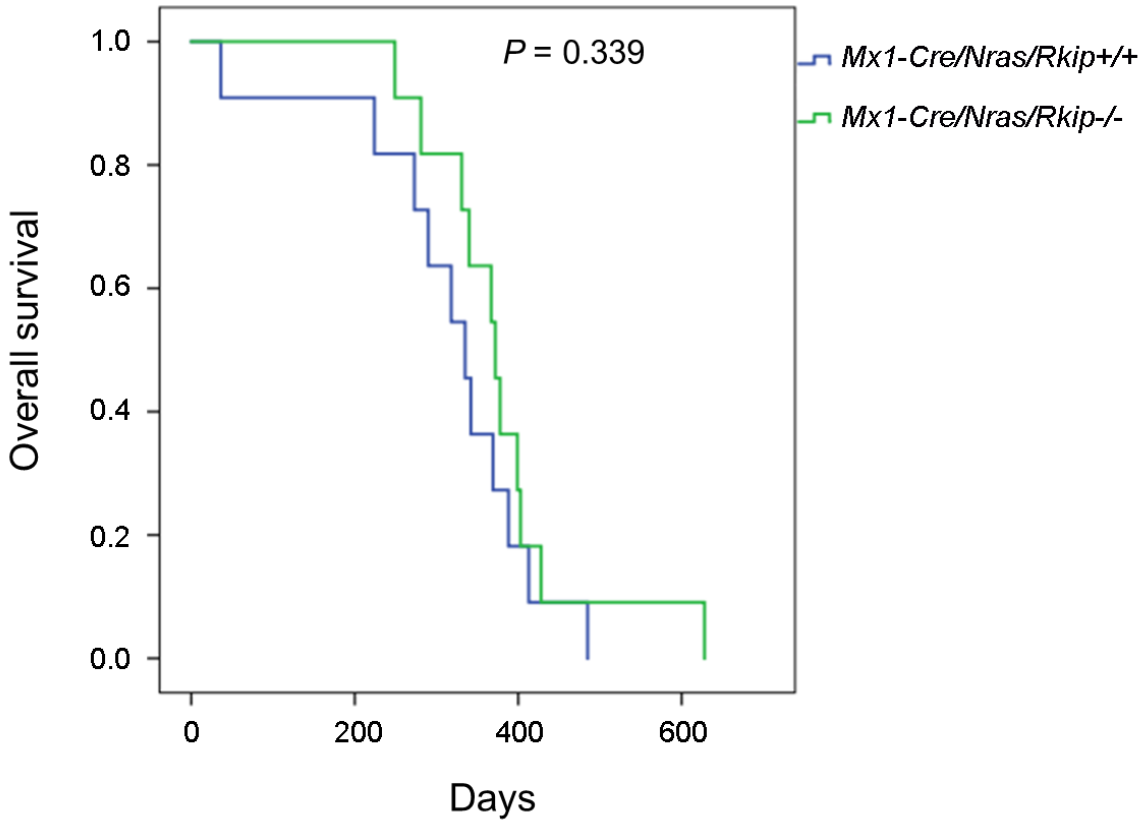

Supplemental Figure 7. Overall survival of *Nras*-mutated mice. *Nras*-mutated mice, with (*Mx1-Cre/Nras/Rkip-/-*; n=11) or without (*Mx1-Cre/Nras/Rkip+/+*, n=11) additional *Rkip* deletion showed no significant difference in the survival rate. A log-rank test was used for these calculations.

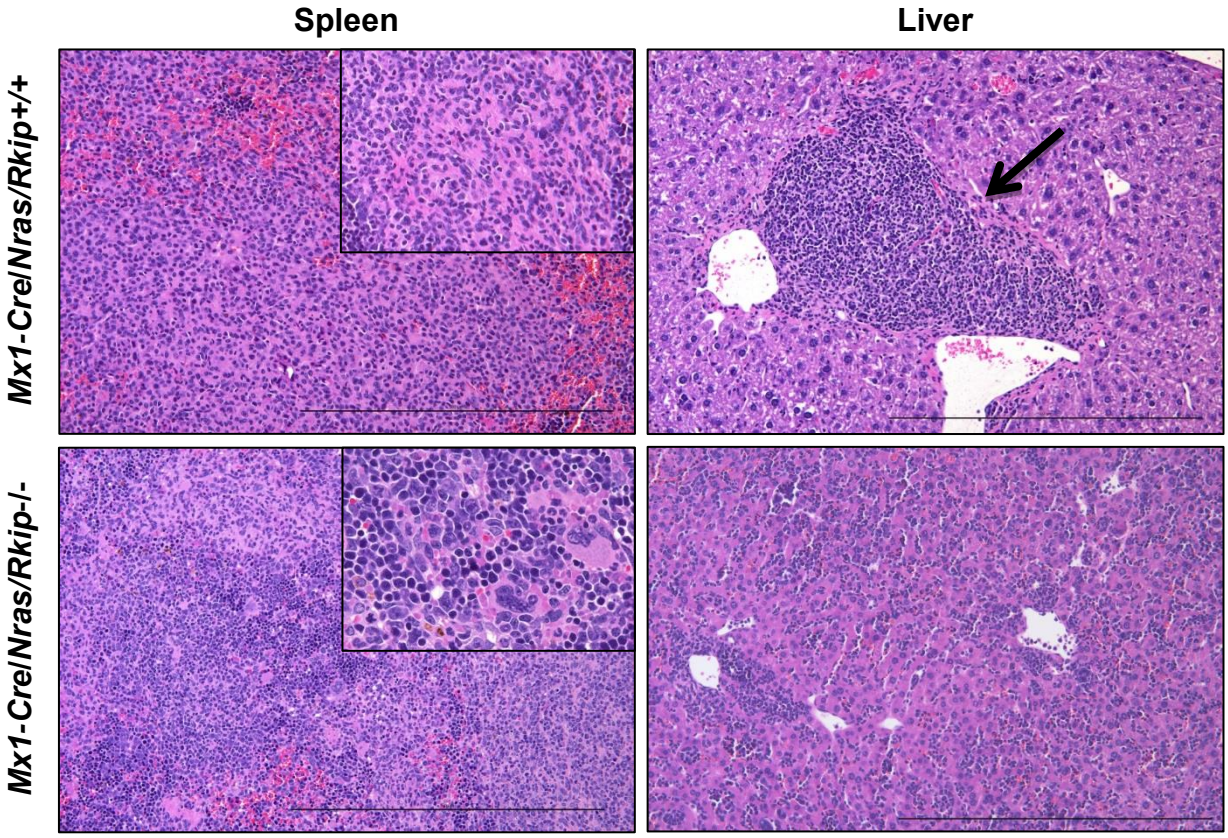

Supplemental Figure 8. Induction of myeloproliferation in *Nras*-mutated mice with *Rkip* deletion coincides with a mitigation of histiocytic sarcoma development. Representative hematoxylin and eosin stained sections of spleen and liver of the mouse genotypes as indicated. Mice were sacrificed when moribund. As in the analyses of mice electively killed at an age of six months after the first pIpC injection, animals with *Rkip* deletion thereby demonstrated an increase in myeloproliferation (as seen in the spleen, bottom left, as well as in the insert, showing multiple megakaryocytes) when compared to the *Rkip*+/+ mice (spleen top left, and insert top left, where almost exclusively histiocytic sarcoma is visible). The formation of histiocytic sarcomas, however, was mitigated in the *Rkip* deleted genotypes as clearly seen in the liver sample (bottom right, only small infiltrates present) compared to the *Rkip*+/+ liver showing an extensive infiltration by histiocytic sarcoma (top right, arrow). The black bar denotes a distance of 500 µm.

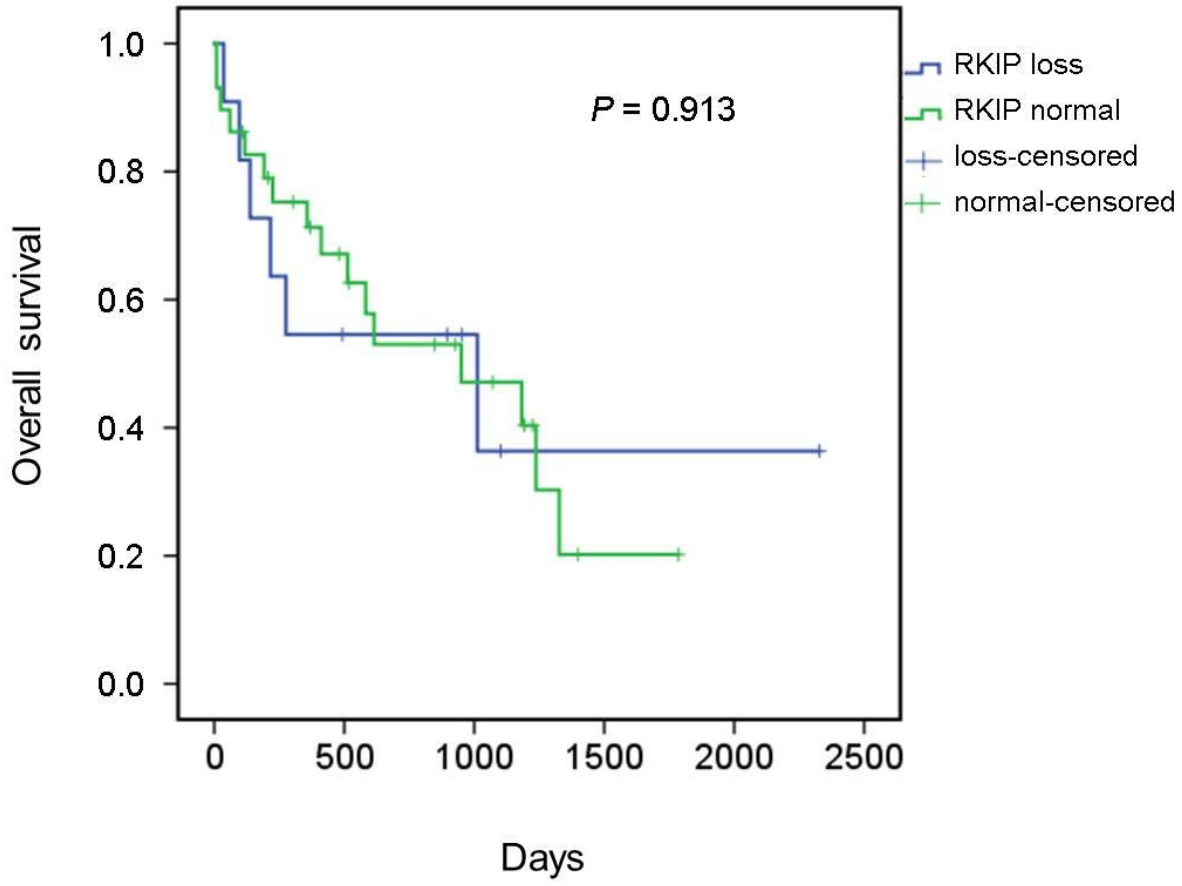

Supplemental Figure 9. Overall survival of CMML patients. No significant differences could be observed in the survival of the CMML patients when comparing patients with RKIP loss (n=12) and those without (n=29). A log-rank test was used for these calculations.

References

1. Wölfler A, Danen-van Oorschot AA, Haanstra JR, et al. Lineage-instructive function of C/EBPα in multipotent hematopoietic cells and early thymic progenitors. Blood 2010;116(20):4116–4125.

2. Caux C, Massacrier C, Dubois B, et al. Respective involvement of TGF-β and IL-4 in the development of Langerhans cells and non-Langerhans dendritic cells from CD34+progenitors. Journal of Leukocyte Biology 1999;66(5):781–791.

3. Zebisch A, Wölfler A, Fried I, et al. Frequent loss of RAF kinase inhibitor protein expression in acute myeloid leukemia. Leukemia 2012;26(8):1842–1849.

4. Schneider CA, Rasband WS, Eliceiri KW. NIH Image to ImageJ: 25 years of image analysis. Nature Methods 2012;9(7):671–675.

5. Caraffini V, Perfler B, Berg JL, et al. Loss of RKIP is a frequent event in myeloid sarcoma and promotes leukemic tissue infiltration. Blood 2018;131(7):826–830.

6. Kashofer K, Gornicec M, Lind K, et al. Detection of prognostically relevant mutations and translocations in myeloid sarcoma by next generation sequencing. Leukemia and Lymphoma 2018;59(2):501–504.

7. Lal R, Lind K, Heitzer E, et al. Somatic TP53 mutations characterize preleukemic stem cells in acute myeloid leukemia. Blood 2017;129(18):2587–2591.

8. Gaksch L, Kashofer K, Heitzer E, et al. Residual disease detection using targeted parallel sequencing predicts relapse in cytogenetically normal acute myeloid leukemia. Am J Hematol 2018;93(1):23–30.

9. Kogan SC, Ward JM, Anver MR, et al. Bethesda proposals for classification of nonlymphoid hematopoietic neoplasms in mice. Blood 2002;100(1):238–245.

10. Lacroix-Triki M, Lacoste-Collin L, Jozan S, Charlet JP, Caratero C, Courtade M. Histiocytic sarcoma in C57BL/6J female mice is associated with liver hematopoiesis: Review of 41 cases. Toxicol Pathol 2003;31(3):304–309.

11. Sung L-Y, Gao S, Shen H, et al. Differentiated cells are more efficient than adult stem cells for cloning by somatic cell nuclear transfer. Nat Genet 2006;38(11):1323–1328.

12. Konuma T, Nakamura S, Miyagi S, et al. Forced expression of the histone demethylase Fbxl10 maintains self-renewing hematopoietic stem cells. Exp Hematol 2011;39(6):697–709.

13. Moran-Crusio K, Reavie L, Shih A, et al. Tet2 loss leads to increased hematopoietic stem cell self-renewal and myeloid transformation. Cancer Cell 2011;20(1):11–24.

14. Wang Y, Krivtsov A V, Sinha AU, et al. The Wnt/β-catenin Pathway Is Required for the Development of Leukemia Stem Cells in AML. Science 2010;327(5973):1650-1653.

15. Escara-Wilke J, Keller JM, Ignatoski KMW, et al. Raf kinase inhibitor protein (RKIP) deficiency decreases latency of tumorigenesis and increases metastasis in a murine genetic model of prostate cancer. Prostate 2015;75(3):292–302.

16. Wang J, Liu Y, Li Z, et al. Endogenous oncogenic NRAS mutation promotes aberrant GM-CSF signaling in granulocytic/monocytic precursors in a murine model of chronic myelomonocytic leukemia. Blood 2010;116(26):5991–6002.

17. Li Q, Haigis KM, McDaniel A, et al. Hematopoiesis and leukemogenesis in mice expressing oncogenic NrasG12D from the endogenous locus. Blood 2011;117(6):2022–2032.